Pergamon

Int. J. Solids Structures Vol. 31, No. 24, pp. 3375–3386, 1994

0020–7683/94 $7.00 + .00

0020–7683(94)00107–3

IDENTIFICATION OF RESPONSE FUNCTIONS FROM AXISYMMETRIC MEMBRANE INFLATION TESTS: IMPLICATIONS FOR BIOMECHANICS

F. P. K. HSU, C. SCHWAB, D. RIGAMONTI and J. D. HUMPHREY

Departments of Mechanical Engineering, Applied Mathematics and Neurological Surgery, The University of Maryland, Baltimore, MD 21228-5398, U.S.A.

(*Received* 14 *September* 1993; *in revised form* 26 *May* 1994)

Abstract—There is a need in biomechanics to identify classes of experiments that allow direct determination of constitutive relations while preserving the natural geometry of the tissue. In this paper, we show how specific forms of response functions can be identified for nonlinear hyperelastic membranes by measuring principal stretch ratios, principal curvatures and distending pressures during quasi-static axisymmetric inflation tests. For completeness, we also list all of the equations that are needed to experimentally implement this new constitutive approach.

INTRODUCTION

There are numerous ways to identify constitutive relations in finite elasticity, but we have found the method proposed by Rivlin and Saunders (1951) to be particularly useful. They showed that specific forms of response functions for nonlinear, incompressible, hyperelastic, isotropic solids can be determined directly from select experiments. Man-made materials, such as elastomers, can usually be fabricated in the requisite geometry, thereby rendering Rivlin's method universally applicable to all materials of that class. In contrast, however, the size and shape of biological tissues is dictated by nature. Since the choice of specimen geometry is often limited, one must seek experiments that can be performed on the tissue of interest and that are well suited for rigorous interpretation.

As an example, consider intracranial saccular aneurysms which are often small, thin-walled, axisymmetric, sac-like structures that are subjected to internal (i.e. blood) and external (cerebrospinal) fluid pressures. Moreover, they often have negligible bending stiffness (Hsu, 1993). Consequently, the most convenient and, probably, most appropriate experiment for quantifying the mechanical properties of these aneurysms is a finite inflation test. Solutions to axisymmetric membrane inflation problems have been known for many years (Green and Adkins, 1970), but no one has shown how, or even if, inflation tests can be used to determine response functions from data consistent with the approach of Rivlin. The purpose of this paper, therefore, is (a) to outline a method for determining functional forms of constitutive relations for nonlinear hyperelastic membranes directly from quasi-static, axisymmetric inflation tests, and (b) to demonstrate the validity of this method through numerical experiments for a membrane having a known strain energy function. Finally, we also catalogue all of the equations that are needed to experimentally implement this new constitutive approach.

METHODS

Theoretical framework

Descriptors of the mechanical behavior of membranes capable of finite deformations are often written in terms of the Cauchy stress resultant tensor $\mathbf{T}$, which is defined as an in-plane force acting over a deformed length (Green and Adkins, 1970; Spencer, 1970). For hyperelastic membranes, there are two basic ways to relate $\mathbf{T}$ to the finite deformations: one can use either a three- or a two-dimensional strain energy function. Herein, we adopt

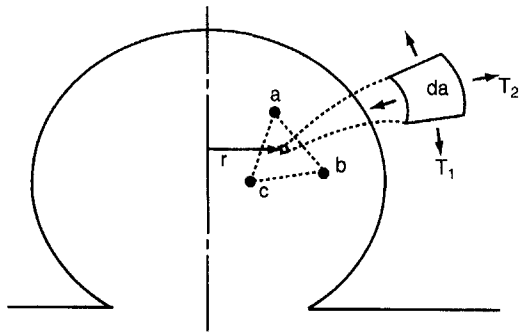

Fig. 1. Schematic of an axisymmetrically inflated membrane showing a region of experimental interest, demarcated by a triplet of markers (a,b,c), in which "measurable" principal stretches and stress resultants T_α are used to calculate response functions. Multiple sets of markers can be used to interrogate material behavior at various locations on the membrane since the stretches and stresses (and thus curvatures) vary from point-to-point in general.

the two-dimensional relation proposed by Humphrey *et al.* (1992a) which is an extension of that suggested by Pipkin (1968). This relation, written in terms of in-plane physical components, is

$$T_{\alpha\beta} = \frac{1}{J} F_{\alpha\Gamma} F_{\beta\Delta} \frac{\partial w}{\partial E_{\Gamma\Delta}}, \quad \alpha, \beta, \Gamma, \Delta = 1, 2, \tag{1}$$

where $J = \det \mathbf{F}$, $\mathbf{F}$ is the two-dimensional deformation gradient tensor, $\mathbf{E}$ [$= 1/2(\mathbf{F}^T\mathbf{F} - \mathbf{I})$] is the two-dimensional Green strain tensor, and w is a strain energy function defined per unit undeformed area.

The only non-zero components of $\mathbf{T}$ and $\mathbf{F}$ in an axisymmetrically inflated membrane, relative to meridional and circumferential directions, are the principal components. Thus, eqn (1) can be solved for the "yet unknown" response functions w_{11} ($= \partial w/\partial E_{11}$) and w_{22} ($= \partial w/\partial E_{22}$), namely

$$w_{11} = \frac{\lambda_2}{\lambda_1} T_1, \quad w_{22} = \frac{\lambda_1}{\lambda_2} T_2, \tag{2}$$

where λ_α are principal stretch ratios (i.e. $\mathbf{F} = \text{diag}[\lambda_1, \lambda_2]$), T_α are principal stress resultants, and "1" and "2" denote meridional and circumferential directions, respectively. Thus, specific forms of response functions w_{11} and w_{22} can be determined *directly* from experimental data, provided that principal stretches (and thus Green strains) and stress resultants can be "measured" at multiple inflation states.

Principal stretch ratios are, of course, easily measured at multiple sites on an inflated membrane by tracking sets of markers that are affixed to the surface of the specimen. For completeness, a method for converting three-dimensional positions of tracked markers into local surface strains is in Appendix A. Moreover, see Hsu (1993) for a description of a video-based system for performing such experiments.

In contrast, principal stress resultants T_α cannot be measured directly. Rather, they must be calculated from the governing differential equations for the quasi-static, axisymmetric inflation of the membrane. These relations are well known and can be written as (Green and Adkins, 1970; Libai and Simmonds, 1988)

$$\frac{\mathrm{d}}{\mathrm{d}r}(rT_1) = T_2, \quad \kappa_1 T_1 + \kappa_2 T_2 = P \tag{3}$$

where r is the location, with respect to the symmetry axis, of a material particle in the deformed configuration (Fig. 1), κ_α are the principal curvatures, and P is the membrane

inflation pressure. Substituting eqn $(3)_1$ into $(3)_2$, invoking the following form of the Gauss–Codazzi relation,

$$\frac{\mathrm{d}}{\mathrm{d}r}(r\kappa_2) = \kappa_1, \tag{4}$$

integrating, and requiring the stress resultants to be finite everywhere, yields the simple results that (Green and Adkins, 1970)

$$T_1 = \frac{P}{2\kappa_2}, \quad T_2 = \frac{P}{\kappa_2}\left(1 - \frac{\kappa_1}{2\kappa_2}\right). \tag{5}$$

Equations (5) reveal that principal stress resultants are also "measurable" provided that the inflation pressure and curvatures are known at the point of interest. For quasi-static inflations, P can be assumed to be uniform within the membrane and hence is easily measured with standard transducers.

Although there are various ways to express the principal curvatures, consider the following relations (Green and Adkins, 1970):

$$\kappa_1 = -\frac{r''}{\sqrt{1-(r')^2}}, \quad \kappa_2 = \frac{\sqrt{1-(r')^2}}{r}, \tag{6}$$

where $r' = \mathrm{d}r/\mathrm{d}\xi$ and ξ is a meridional arc length in the deformed configuration. Hence, "measuring" principal curvatures only requires that one determine a C^2 function $r = r(\xi)$, which is easily constructed via an interpolation of positions of multiple points along a contour of the inflating membrane. This interpolation can be accomplished in many different ways, but for completeness we outline one possible method in Appendix B.

In summary, response functions for nonlinear membranes can be determined directly from measurable principal stretches, principal curvatures, and the inflation pressure, namely

$$w_{11} = \frac{\lambda_2}{\lambda_1}\left(\frac{P}{2\kappa_2}\right), \quad w_{22} = \frac{\lambda_1}{\lambda_2}\left(\frac{P}{\kappa_2}\right)\left(1 - \frac{\kappa_1}{2\kappa_2}\right), \tag{7}$$

at various sites on the membrane and at multiple quasi-statically inflated configurations. To illustrate the potential utility of this new approach, we now present results from simulations using a known two-dimensional strain energy function.

Numerical experiments

Consider an initially flat, circular membrane (with initial outer radius ρ_o) that is clamped around its periphery and pressurized from underneath. Moreover, let the membrane be a STZC material, and hence described by a strain energy function of the form (Skalak *et al.*, 1973)

$$w = \frac{c_1}{8}(I_1^2 + 2I_1 - 2I_2 + \Gamma I_2^2), \tag{8}$$

where $\Gamma = c_2/c_1$, c_1 and c_2 are material parameters, $I_1 = 2(E_{11} + E_{22})$, and $I_2 = 4E_{11}E_{22} + 2(E_{11} + E_{22})$. For purposes of illustration, and ease of comparison to results in the literature, we let the magnitudes of ρ_o, c_1 and c_2 each equal unity in the simulations below; ρ_o and c_1 were used further to non-dimensionalize all numerical results (Figs 2–7).

Different methods have been proposed to solve membrane inflation problems [e.g. Adkins and Rivlin (1952); Klingbeil and Shield (1964); Yang and Feng (1970); Wu (1979)], but we followed Hart-Smith and Crisp (1967) and Schmidt and Carley (1975), with slight

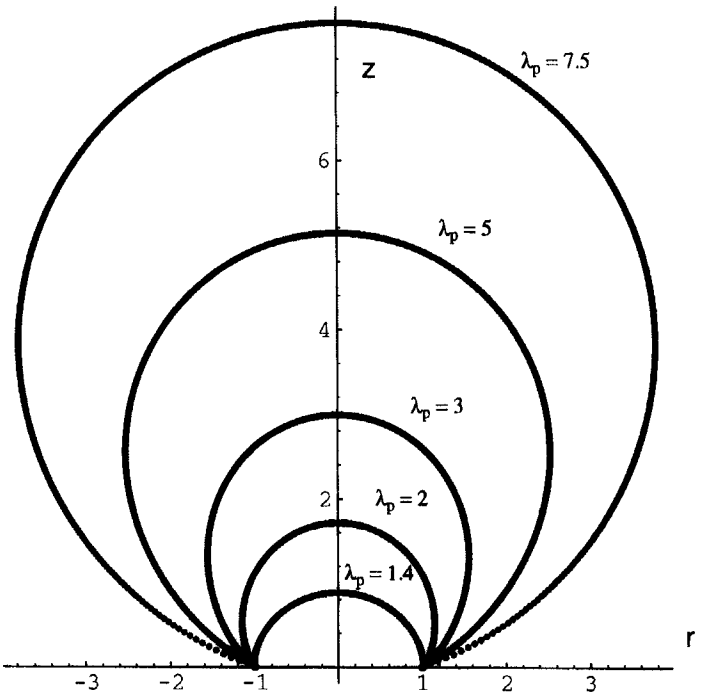

Fig. 2. Profiles of an initially flat STZC membrane [i.e. defined by the strain energy in eqn (8)] at five different inflated configurations: $\lambda_p = \sqrt{2}$, 2, 3, 5 and 7.5 where λ_p is the equibiaxial stretch at the pole. The membrane is clamped at its base.

modifications. Briefly, the governing equations at each quasi-static equilibrium configuration m reduce to a set of first-order ordinary differential equations parameterized by the undeformed radial coordinate ρ. These equations were numerically integrated by a standard, explicit two-stage Runge–Kutta scheme. A detailed outline of our computational algorithm is in Appendix C, but note that the solution began at the pole p of the membrane by prescribing a value for the principal stretches $\lambda_1 = \lambda_2 = \lambda_p$, and then calculating the associated (i.e. at p) principal curvatures $\kappa_1 = \kappa_2 = \kappa_p$, principal stress resultants $T_1 = T_2 = T_p$, and inflation pressure P. Requisite derivatives were then calculated at the pole and subsequently at all locations from the pole to the clamped edge $\rho = \rho_o$.

RESULTS

Results were first calculated for $m = 7$ inflation configurations: $\lambda_p = \sqrt{2}$, 2, 3, 4, 5, 7.5 and 10. For clarity, we show associated membrane profiles for only five of these configurations (Fig. 2); they compare well with results obtained by Pujara and Lardner (1978) for a similar problem. That the membrane was nearly spherical at $\lambda_p = 10$ was one reason for otherwise arbitrarily selecting this value as the upper bound. The principal values of the stretch ratios, curvatures and stress resultants are shown in Fig. 3 as a function of the undeformed radial location ρ; panels A–C show complete results for $\lambda_p = \sqrt{2}$ whereas panels D–F show results for $\lambda_p = 5$.

Consider the case where $\lambda_p = \sqrt{2}$. As required, values of λ_α, κ_α and T_α were each equal at the pole, and $\lambda_2 \equiv 1$ at $\rho = 1$ (i.e. ρ_o). Moreover, all six quantities changed monotonically from the pole to the clamped base; T_1 decreased slightly near the base despite an increasing λ_1. Results for $\lambda_p = 5$ were dramatically different. In particular, note the change of scale in the ordinate in panels D and F and that curvatures and stress resultants did not change monotonically. There were also steep gradients in T_2 and κ_1 near the edge (i.e. a boundary layer phenomenon), but consistent with a more spherical shape, curvatures and stress resultants were each nearly equal in the upper half of the membrane. Though not shown, these findings were even more remarkable when $\lambda_p \geqslant 7.5$.

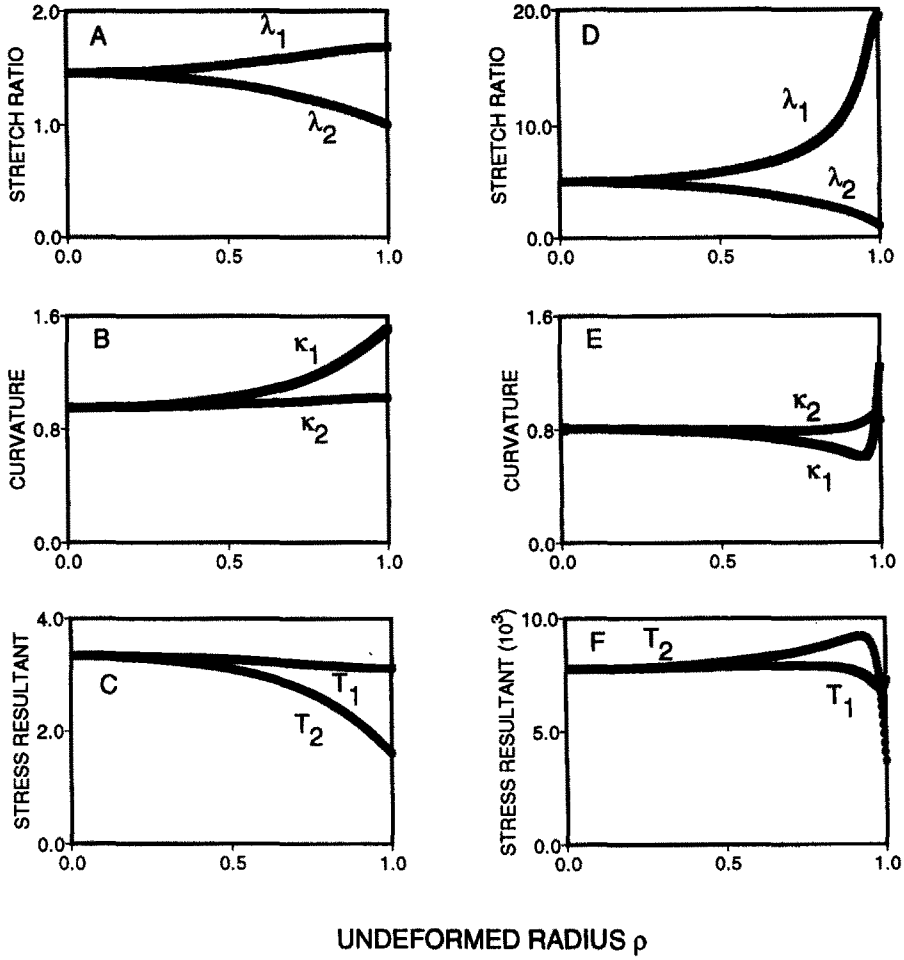

Fig. 3. Calculated principal stretches (panels A, D), curvatures (B, E) and stress resultants (C, F) for an inflated STZC membrane, each plotted versus undeformed radial location for two configurations: panels A–C are for a pole stretch ratio of $\lambda_p = \sqrt{2}$ whereas D–F are for $\lambda_p = 5$. Note the different scales in the ordinates.

Since these solutions provide complete information on principal stretches, curvatures and stress resultants at every point on the pressurized membrane, we could determine values of the response functions (directly from data) anywhere on the membrane. For purposes of illustration, we show "measured" response functions from $m = 9$ configurations ($\lambda_p = 1.2, 1.3 \ldots 2.0$) at three different locations: $\rho = 0$ (i.e. the pole), $\rho = 0.5$ and $\rho = 1$ (i.e. the base). Specifically, the inflation pressure is plotted versus the principal curvatures and Green strains in Fig. 4; panels A and D are at $\rho = 0$, B and E at $\rho = 0.5$, and C and F at $\rho = 1$. Since $\lambda_1 = \lambda_2$ at the pole, data from this location can be thought of as being from an "equibiaxial stretching test". Conversely, $\lambda_2 \equiv 1$ at the base, hence data from this location can be thought of as being from a "strip biaxial" or shear test. Lastly, data at $\rho = 0.5$ can be thought of as being from a proportional stretching or "off-biaxial" test. These observations are seen in Fig. 4, panels D, F and E, respectively; similar observations were pointed out previously by Wineman *et al.* (1979).

Finally, and most importantly, we show values of the response functions w_{11} and w_{22} plotted versus the principal Green strains E_{11} and E_{22} in Figs 5, 6 and 7 for data from Figs 4A and D, B and E, and C and F, respectively. Figs 5A–D reveal that both response functions are mildly nonlinear, they depend on both of the principal strains, they increase monotonically with increasing strain, and they tend to zero at zero strain. Moreover, since $E_{11} = E_{22}$ in Fig. 5, the identical results for w_{11} versus E_{11} and E_{22}, and w_{22} versus E_{22} and E_{11} suggest that the material is isotropic, that is $w(E_{11}, E_{22}) = w(E_{22}, E_{11})$. Figure 7 reveals further that, for constant E_{22} ($= 0$), w_{11} is nearly linear in E_{11} with a zero intercept, whereas

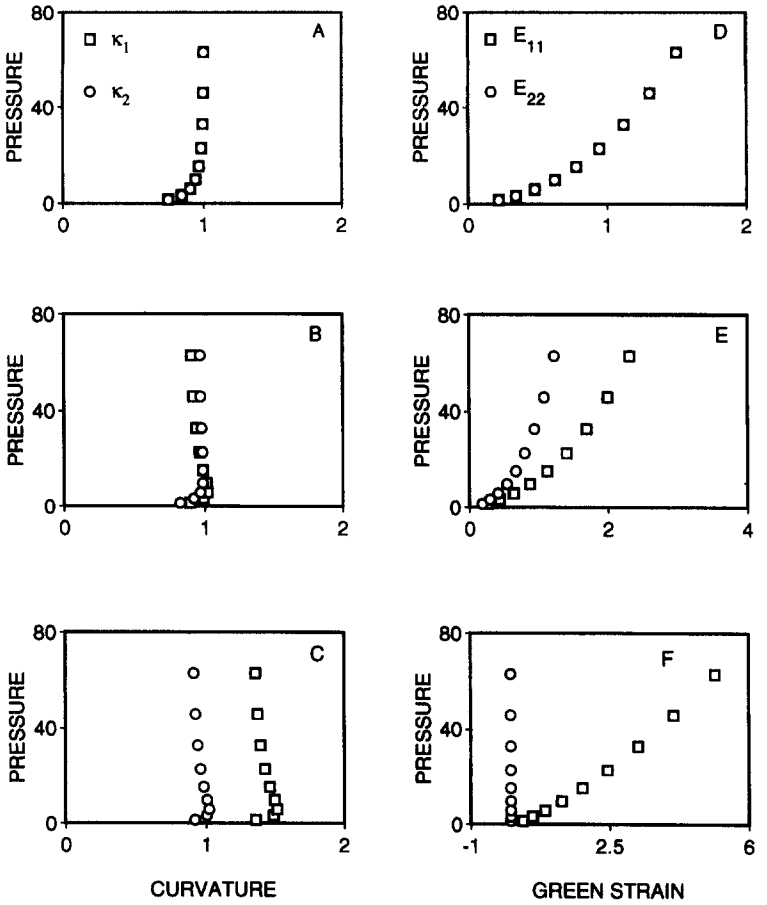

Fig. 4. Inflation pressure P versus principal curvatures (panels A–C) and principal Green strains (D–F) for nine quasi-statically inflated configurations ($\lambda_p = 1.2, 1.3 \ldots 2.0$). Moreover, "data" are given at three locations on the membrane: panels A and D are from the pole ($\rho = 0$), panels B and E are from $\rho = 0.5$, and panels C and F are from the clamped base ($\rho = 1$). Note the equibiaxial stretch at the pole, proportional stretch in the "middle" of the membrane, and strip biaxial stretch (i.e. $E_{22} \equiv 0$) at the base.

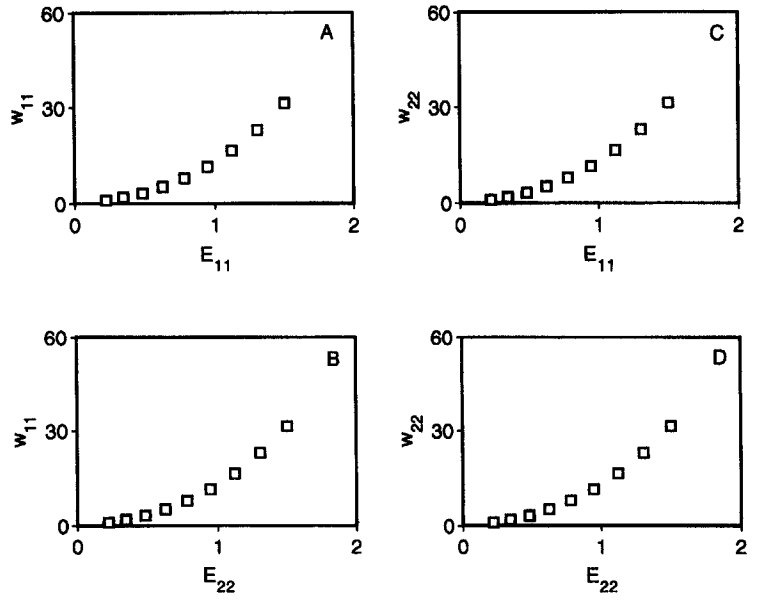

Fig. 5. Plots of the response functions w_{11} and w_{22} calculated at the pole (i.e. $\rho = 0$) from the nine quasi-static inflation states shown in Fig. 4. Note that w_{11} versus E_{11} and E_{22}, and w_{22} versus E_{11} and E_{22}, are the same, thereby revealing an isotropic response to equibiaxial stretching.

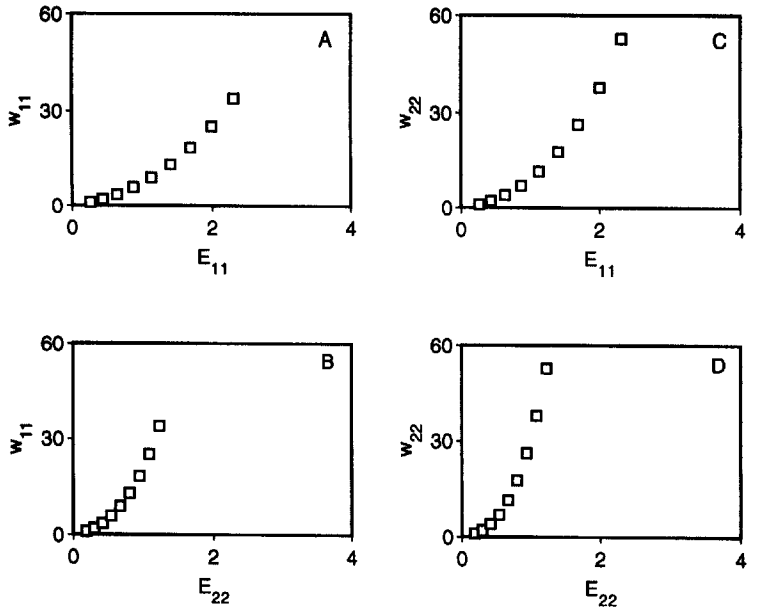

Fig. 6. The same as Fig. 5, except that the response functions were calculated from data at a different location on the membrane (i.e at $\rho = 0.5$).

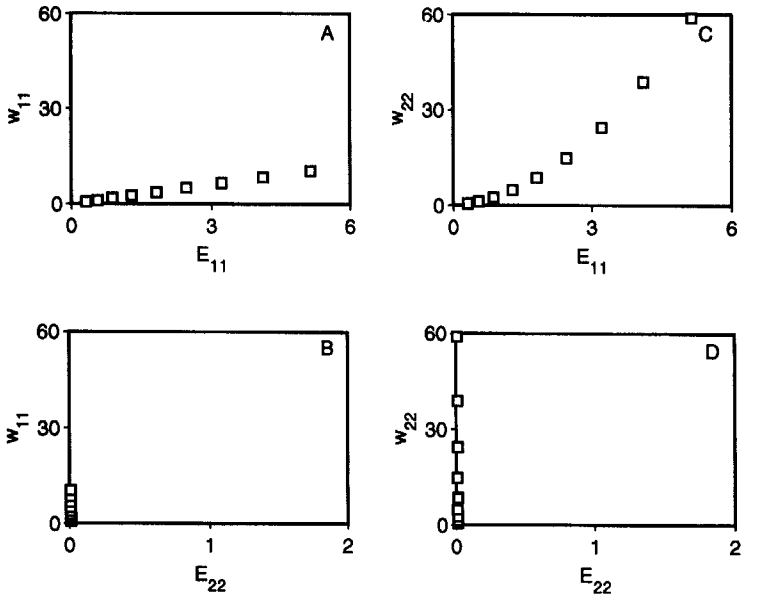

Fig. 7. The same as Figs 5 and 6, except that the response functions were calculated from data at a different location on the membrane (i.e. at the clamped base where $\rho = 1.0$ and $\lambda_2 \equiv 1$). Note that w_{11} appears to be linear in E_{11} whereas w_{22} appears to be nonlinear in E_{11}.

w_{22} is nonlinear in E_{11} but approaches zero as E_{11} tends to zero. Since Fig. 5 suggests an isotropic behavior, similar findings would be expected for constant E_{11} tests which, of course, cannot be realized in this membrane inflation test. Finally, data in Fig. 6 confirms that the response functions depend proportionately on both strains. Clearly, these observations, direct from "data", provide tremendous insight into reasonable forms of response functions for this material. Moreover, though not shown, these data can also provide important information on material parameters [e.g. by *empirical-inequalities*; see Truesdell and Noll (1965)] once specific forms of these relations are identified [see, Rivlin and Saunders (1951); Humphrey *et al.* (1990, 1992a)].

Finally, writing out the response functions for eqn (8) in terms of $E_{\Gamma\Delta}$ allows one to appreciate better that observations from Figs 5–7 reflect the true material behavior well. For example, by writing the response functions as

$$w_{11} = (c_1+c_2)E_{11}+c_2E_{22}+4c_2E_{11}E_{22}+2c_2E_{22}^2+4c_2E_{11}E_{22}^2 \tag{9}_1$$

and

$$w_{22} = (c_1+c_2)E_{22}+c_2E_{11}+4c_2E_{11}E_{22}+2c_2E_{11}^2+4c_2E_{22}E_{11}^2 \tag{9}_2$$

we can see that observations from Fig 5 are correct. Similarly, if we rearrange eqns $(9)_{1-2}$ as follows,

$$w_{11} = [c_2E_{22}+2c_2E_{22}^2]+[c_1+c_2+4c_2E_{22}+4c_2E_{22}^2]\,E_{11} \tag{9}_3$$

and

$$w_{22} = [(c_1+c_2)E_{22}]+[c_2+4c_2E_{22}]\,E_{11}+[2c_2+4c_2E_{22}]E_{11}^2, \tag{9}_4$$

it is easy to see that observations from Fig. 7 are also correct.

DISCUSSION

Constitutive formulations

To exploit the tremendous advances in computational mechanics, one must have reliable descriptions of the mechanical behavior of the materials of interest. In general, there are three ways to identify a mechanical constitutive relation. First, one can formulate a relation based on theoretical considerations (e.g. statistical mechanics) of the microstructure of the material. Although this is perhaps the best approach in principle, the complex, composite constitution of many elastomers and biosolids necessitate many simplifying assumptions, ramifications of which are difficult to evaluate. Second, one can "guess" forms of constitutive relations based on gross observations of material behavior, experience with similar materials, or mathematical convenience (e.g. specific expansions of W in terms of strains). Many useful relations have been, and will likely continue to be, formulated in this way. Nonetheless, it is difficult to determine if "guessed" relations are optimal.

Third, it is possible to identify specific forms of response functions and realistic ranges of the values of the material parameters *directly* from experimental data. This approach is particularly appealing since it is the material itself that guides the formulation. To employ this approach, however, one must obtain analytical, universal solutions to boundary value problems that correspond to tractable experiments. Due to the difficulty of solving problems in finite elasticity, only a few such solutions are available. Rivlin and Saunders (1951) showed that the form of the response functions for nonlinear, incompressible, hyperelastic isotropic solids could be identified directly from in-plane biaxial tests on thin, flat specimens. Penn and Kearsley (1976) and Storakers (1979) showed that finite extension and torsion tests on isotropic solid circular specimens can yield similar information. More recently, Humphrey *et al.* (1990, 1992a,b) showed that in-plane biaxial and combined extension–torsion tests can also be used to identify response functions for a sub-class of nonlinear, incompressible, transversely isotropic solids, and that in-plane biaxial tests can yield similar information on nonlinearly hyperelastic membranes.

Utility of membrane tests

Classes of experiments available to identify response functions for nonlinear solids are limited therefore, but this has not been a serious problem in studying man-made materials since specimens can usually be fabricated in the requisite shape. As previously mentioned, this is not necessarily true for biosolids; nature dictates the size and shape of tissues and

cells, which often precludes the experimentalist from obtaining specimens suitable for in-plane biaxial or combined extension–torsion experiments—intracranial saccular aneurysms are a good example of such tissues.

Indeed, like many soft tissues, saccular aneurysms are more conveniently and appropriately tested via finite strain inflation experiments. Methods for solving quasi-static, finite, axisymmetric inflations of membranes (having a known constitutive relation) have been available for many years, but we have shown for the first time that the functional form of the response functions can be inferred directly from such experiments. Of course, once response functions are identified, inflation tests can also be used to determine "best-fit" values of the associated material parameters; this has been the primary use of inflation tests heretofore [e.g. Klingbeil and Shield, (1964); Schmidt and Carley (1975); Wineman *et al.* (1979); Kriewall *et al.* (1983); Bylski *et al.* (1986)].

Another advantage of inflation tests is that data collected from multiple sites on a homogenous membrane actually yield information corresponding to different multiaxial experimental protocols (Wineman *et al.*, 1979). This was illustrated in Figs 4D, E and F which correspond to equibiaxial, proportional and strip biaxial stretching tests, respectively. This may prove to be important in studying elastomeric and biosolid materials which exhibit history-dependent behavior (e.g. Mullin's effect and preconditioning, respectively). That is, because multiple experimental protocols are needed to provide data sufficient to fully quantify material behavior and evaluate the predictive capability of the final constitutive relation, and because the behavior of these materials can change with repeated loading (e.g. sequential protocols), inflation tests may provide new insights into these materials since "multiple protocols" can be performed simultaneously. Finally, inflated membranes often fail at the pole, and hence are convenient for evaluating rupture (i.e. failure) properties.

Limitations of membrane tests

In addition to requiring slightly more involved methods of data collection and reduction (as compared to in-plane biaxial and torsion tests), the primary limitation of membrane inflation tests is the inability to separately control the two principal strains or stresses. For example, independent control of orthogonal extensions during in-plane biaxial tests allows one to perform tests wherein one coordinate invariant measure of the finite deformation is maintained constant while the other varies, and vice versa. These so-called "constant invariant tests" are particularly useful in studying the behavior of both isotropic and transversely isotropic solids (Rivlin and Saunders, 1951; Humphrey *et al.*, 1990).

The utility of separately maintaining one principal extension constant while the other varies, and vice versa, is also illustrated in Fig. 7 and by eqns $(9)_{3,4}$. Clearly, being able to generate families of response functions by separately maintaining extensions constant at different values can be very beneficial (Humphrey *et al.*, 1992a). Unfortunately, there is only one location on an inflated membrane where one extension can be kept constant while the other varies ($\lambda_2 \equiv 1$ at the clamped base), and data at this location are unlikely to be useful. That is, at the clamp, one must contend with experimental "edge effects" and steep gradients due to a boundary layer phenomena (Wu and Perng, 1972), both of which make it difficult to accurately measure κ_1, κ_2 and λ_1. Finally, the inability to investigate a wide range of shear behavior using inflation tests is a shortcoming, which is common to the in-plane biaxial test. Other related experimental configurations [e.g. Feng and Yang (1973); Bylski *et al.* (1986)] may provide additional protocols, but this requires further study.

Closure

Despite some limitations, quasi-static, axisymmetric inflation tests promise to provide information that otherwise would not be available to guide the formulation of constitutive relations for nonlinearly hyperelastic membranes that cannot be subjected to other, more traditional tests.

Acknowledgements—Partial financial support from the Veterans Affairs Medical Center, Baltimore (to DR and JDH), the National Science Foundation through Grant PYI:BCS-9157798 (to JDH), and the Air Force Office of Scientific Research through Grant F49620-J-0100 (to CS) is gratefully acknowledged.

REFERENCES

Adkins, J. E. and Rivlin, R. S. (1952). Large elastic deformations of isotropic materials. IX. The deformations of thin shells. *Phil. Trans. R. Soc.* **244A,** 505–531.

Bylski, D. I., Kriewall, T. J., Akkas, N. and Melvin, J. W. (1986). Mechanical behavior of fetal dura mater under large deformation biaxial tension. *J. Biomech.* **19,** 19–26.

Feng, W. W. and Yang, W. H. (1973). On the contact problem of an inflated spherical nonlinear membrane. *J. Appl. Mech.* **40,** 209–214.

Green, A. E. and Adkins, J. E. (1970). *Large Elastic Deformations.* Clarendon Press, Oxford.

Hart-Smith, L. J. and Crisp, J. D. C. (1967). Large elastic deformations of thin rubber membranes. *Int. J. Engng Sci.* **5,** 1–24.

Hsu, P. P. K. (1993). Material identification using membrane inflation tests: application to saccular aneurysms. Ph.D. Thesis, University of Maryland, Baltimore.

Humphrey, J. D., Strumpf, R. K. and Yin, F. C. P. (1990). Determination of a constitutive relation for passive myocardium. I. A new functional form. *J. Biomech. Engng* **112,** 333–339.

Humphrey, J. D., Strumpf, R. K. and Yin, F. C. P. (1992a). A constitutive theory for biomembranes: application to epicardial mechanics. *J. Biomech. Engng* **114,** 461–466.

Humphrey, J. D., Barazotto, R. L. and Hunter, W. C. (1992b). Finite extension and torsion of papillary muscles: a theoretical framework. *J. Biomech.* **25,** 541–547.

Klingbeil, W. W. and Shield, R. T. (1964). Some numerical investigations on empirical strain energy functions in the large axisymmetric extensions of rubber membranes. *ZAMP* **15,** 608–629.

Kriewall, T. J., Akkas, N., Bylski, D. I., Melvin, J. W. and Work, B. A. (1993). Mechanical behavior of fetal dura mater under large axisymmetric inflation. *J. Biomech. Engng* **105,** 71–76.

Libai, A. and Simmonds, J. G. (1988). *The Nonlinear Theory of Elastic Shells.* Academic Press, New York.

McCulloch, A. D., Smaill, B. H. and Hunter, P. J. (1987). Left ventricular epicardial deformation in isolated arrested dog heart. *Am. J. Physiol.* **252,** 233–241.

Penn, R. W. and Kearsley, E. A. (1976). The scaling law for finite torsion of elastic cylinders. *Trans. Soc. Rheol.* **20,** 227–238.

Pipkin, A. C. (1968). Integration of an equation in membrane theory. *ZAMP* **19,** 818–819.

Pujara, P. and Lardner, T. J. (1978). Deformations of elastic membranes—effect of different constitutive relations. *ZAMP* **29,** 315–327.

Rivlin, R. S. and Saunders, D. W. (1951). Large elastic deformations of isotropic materials. VII. Experiments on the deformation of rubber. *Phil. Trans. R. Soc.* **243A,** 251–288.

Schmidt, L. R. and Carley, J. F. (1975). Biaxial stretching of heat-softened plastic sheets using an inflation technique. *Int. J. Engng Sci.* **13,** 563–578.

Skalak, R., Tozeren, A., Zarda, A. P. and Chien, S. (1973). Strain energy function of red blood cell membranes. *Biophys. J.* **13,** 245–264.

Spencer, A. J. M. (1970). The static theory of finite elasticity. *J. Inst. Math. Applic.* **16,** 164–200.

Storakers, B. (1979). An explicit method to determine response coefficients in finite elasticity. *J. Elasticity* **9,** 207–214.

Truesdell, C. and Noll, W. (1965). The nonlinear field theories of mechanics. In *Handbuch der Physik* (Edited by S. Flugge). Springer-Verlag, Berlin.

Wineman, A., Wilson, D. and Melvin, J. W. (1979). Material identification of soft tissue using membrane inflation. *J. Biomech.* **12,** 841–850.

Wu, C. H. (1979). Large finite strain membrane problems. *Quart. Appl. Math.* **36,** 347–359.

Wu, C. H. and Perng, D. Y. P. (1972). On the asymptotically spherical deformations of arbitrary membranes of revolution fixed along an edge and inflated by large pressures—a nonlinear boundary layer phenomenon. *SIAM J. Appl. Math.* **23,** 133–152.

Yang, W. H. and Feng, W. W. (1970) On axisymmetric deformations of nonlinear membranes. *J. Appl. Mech.* **37,** 1002–1011.

APPENDIX A

It is straightforward to infer in-plane (i.e. two-dimensional) components of the deformation gradient tensor **F** from the three-dimensional position histories of small, closely spaced markers that are affixed to the surface of a deforming membrane. For example, McCulloch *et al.* (1987) reported the following relations based on motions of triplets of markers:

$$F_{11} = \frac{(x_1^b - x_1^a)(X_2^C - X_2^A) - (x_1^c - x_1^a)(X_2^B - X_2^A)}{\mathrm{DET}} \tag{A1}$$

$$F_{12} = \frac{(x_1^c - x_1^a)(X_1^B - X_1^A) - (x_1^b - x_1^a)(X_1^C - X_1^A)}{\mathrm{DET}} \tag{A2}$$

$$F_{21} = \frac{(x_2^b - x_2^a)(X_2^C - X_2^A) - (x_2^c - x_2^a)(X_2^B - X_2^A)}{\mathrm{DET}} \tag{A3}$$

$$F_{22} = \frac{(x_2^c - x_2^a)(X_1^B - X_1^A) - (x_2^b - x_2^a)(X_1^C - X_1^A)}{\mathrm{DET}} \tag{A4}$$

in which A, B, C and a, b, c denote the three markers that constitute a triplet in undeformed and deformed configurations, respectively, and

$$\mathrm{DET} = (X_2^{\mathrm{C}} - X_2^{\mathrm{A}})(X_1^{\mathrm{B}} - X_1^{\mathrm{A}}) - (X_2^{\mathrm{B}} - X_2^{\mathrm{A}})(X_1^{\mathrm{C}} - X_1^{\mathrm{A}}). \tag{A5}$$

X_α^{j} and x_α^{j} are locations of marker j in undeformed and deformed configurations, respectively, both relative to local monoclinic coordinate systems. Equations (A1)–(A4) provide mean values of $F_{\alpha\Gamma}$ within the region demarcated by the triplet, and can be taken as values near the centroid (Fig. 1). The principal values of **F** needed in eqn (2) are thereby "measurable" at a point of interest.

APPENDIX B

Here, we present an interpolation scheme for calculating principal curvatures in an inflated membrane directly from the experimentally measurable surface profile. Let the digitized profile be represented by a finite set of points $\{r_i, z_i\}$, with $i = 1,2\ldots n$, at each inflation configuration m. Moreover, let t_k denote an interpolation parameter which is a rough approximation of an arc length:

$$t_k = t_{k-1} + d_k, \quad k = 2\ldots n, \tag{B1}$$

where

$$t_1 = 0, \quad d_k = \sqrt{(\Delta r_k)^2 + (\Delta z_k)^2} \tag{B2}$$

and

$$\Delta r_k = r_k - r_{k-1}, \quad \Delta z_k = z_k - z_{k-1}. \tag{B3}$$

Next, construct interpolation functions using cubic splines, such that

$$\{t_k, r_k\} \to r(t), \quad \{t_k, z_k\} \to z(t) \tag{B4}$$

and define the arc length $\xi(t)$ as

$$\xi(t) = \int_0^t \sqrt{(\dot{r})^2 + (\dot{z})^2}\, \mathrm{d}t, \tag{B5}$$

where $(\dot{})$ denotes differentiation with respect to the parameter t. Finally, using the chain rule,

$$r' = \frac{\dot{r}}{\sqrt{(\dot{r})^2 + (\dot{z})^2}} \tag{B6}$$

and

$$r'' = \frac{\dot{z}(\dot{z}\ddot{r} - \dot{r}\ddot{z})}{[(\dot{r})^2 + (\dot{z})^2]^{2/3}}, \tag{B7}$$

where r' and r'' are used to calculate the principal curvatures in eqns (7).

APPENDIX C

Here we outline an algorithm for calculating values of the principal stretches, curvatures and stress resultants in an inflated membrane having a known strain energy function [see eqn (3) for the governing differential equation]. The solution is initiated at the pole of the membrane (i.e. location $n = 1$ denoted by p) by prescribing a value for the principal stretches $\lambda_1 = \lambda_2 = \lambda_p$, and then calculating the associated principal curvatures $\kappa_1 = \kappa_2 = \kappa_p \simeq (2/\lambda_p)\sqrt{(\lambda_p - 1)}$, the principal stress resultants $T_1 = T_2 = T_p$ from a constitutive relation [e.g. eqns (1) and, for example, (8)], and the inflation pressure from equilibrium ($P = 2\kappa_p T_p$). Next, the following derivatives are calculated at the pole and subsequently at all locations $n > 1$ from the pole to the clamped edge where $\rho = \rho_o$:

$$\left(\frac{\mathrm{d}r}{\mathrm{d}\rho}\right)_n = \pm(\lambda_1)_n[1 - (\kappa_2 r)^2]_n^{1/2} \tag{C1}$$

$$\left(\frac{\mathrm{d}z}{\mathrm{d}\rho}\right)_n = (\lambda_1 \kappa_2 r)_n \tag{C2}$$

$$\left(\frac{\mathrm{d}\kappa_2}{\mathrm{d}\rho}\right)_n = \left(\frac{\kappa_1 - \kappa_2}{r}\right)_n \left(\frac{\mathrm{d}r}{\mathrm{d}\rho}\right)_n. \tag{C3}$$

When all quantities are known at location n, they are then calculated, *in the following order*, at location $n+1$ via increments $\Delta\rho$ in the undeformed radial location. That is, we first find

$$(r)_{n+1} = (r)_n + \left(\frac{dr}{d\rho}\right)_n \Delta\rho \tag{C4}$$

$$(z)_{n+1} = (z)_n + \left(\frac{dz}{d\rho}\right)_n \Delta\rho \tag{C5}$$

$$(\kappa_2)_{n+1} = (\kappa_2)_n + \left(\frac{d\kappa_2}{d\rho}\right)_n \Delta\rho \tag{C6}$$

and then calculate

$$(\lambda_2)_{n+1} = \left(\frac{r}{\rho}\right)_{n+1} \tag{C7}$$

$$(T_1)_{n+1} = \left(\frac{P}{2\kappa_2}\right)_{n+1} \tag{C8}$$

$$(\lambda_1)_{n+1} = \frac{3^{1/3}(c_1 + c_2\lambda_2^2) + (9c_1\lambda_2\sqrt{c_1 + c_2\lambda_2^4}T_1 + \sqrt{3\Xi})^{2/3}}{3^{2/3}\sqrt{c_1 + c_2\lambda_2^4}(9c_1\lambda_2\sqrt{c_1 + c_2\lambda_2^4}T_1 + \sqrt{3\Xi})^{1/3}} \tag{C9}$$

where

$$\Xi = c_1^3(27\lambda_2^2T_1^2 - 1) + c_1^2c_2(27\lambda_2^6T_1^2 - 3\lambda_2^2) - c_1c_2^2(3\lambda_2^4) - c_2^3(\lambda_2^6)$$

$$(T_2)_{n+1} = \left(\frac{c_1\lambda_2}{2\lambda_1}\right)_{n+1} [\lambda_2^2 - 1 + \Gamma(\lambda_1^4\lambda_2^2 - \lambda_1^2)]_{n+1} \tag{C10}$$

$$(\kappa_1)_{n+1} = (\kappa_2)_{n+1}\left(2 - \frac{T_2}{T_1}\right)_{n+1}. \tag{C11}$$

Note that eqns (C9)–(C10) depend on the particular strain energy function, which in this example is eqn (8). Moreover, eqn (C9) results from solving $T_1 = (\lambda_1/\lambda_2)w_{11}$ for λ_1 in terms of T_1, λ_2 and the material parameters.

An iterative correction is made by evaluating eqns (C1)–(C3) at $n+1$ and then recalculating eqns (C4)–(C6) as follows:

$$(r)_{n+1} = (r)_n + \left[\left(\frac{dr}{d\rho}\right)_n + \left(\frac{dr}{d\rho}\right)_{n+1}\right]\frac{\Delta\rho}{2} \tag{C12}$$

$$(z)_{n+1} = (z)_n + \left[\left(\frac{dz}{d\rho}\right)_n + \left(\frac{dz}{d\rho}\right)_{n+1}\right]\frac{\Delta\rho}{2} \tag{C13}$$

$$(\kappa_2)_{n+1} = (\kappa_2)_n + \left[\left(\frac{d\kappa_2}{d\rho}\right)_n + \left(\frac{d\kappa_2}{d\rho}\right)_{n+1}\right]\frac{\Delta\rho}{2}. \tag{C14}$$

This, in turn, allows calculation of corrected values of T_α, λ_α and κ_1 at location $n+1$. This entire procedure [eqns (C1)–(C14)] is repeated until the deformed and undeformed radii equal one another, that is the solution reaches the outermost particle where $r_f = \rho_f$. Note that $\rho_f \neq \rho_o$, in general, since this boundary value problem is solved as an "initial value problem". Equations (3) admit a family of similarity solutions, however, one can pick that solution which satisfies the boundary condition $r_o/\rho_o = 1$. This is accomplished via an appropriate scaling of the computed solution (Klingbeil and Shield, 1964; Yang and Feng, 1970; Schmidt and Carley, 1975), as for example:

$$\hat{\rho} = \frac{\rho}{\rho_f}, \quad \hat{r} = \frac{r}{\rho_f}, \quad \hat{T}_\alpha = \frac{T_\alpha}{\rho_f}, \quad \hat{\kappa}_\alpha = \rho_f\kappa_\alpha, \quad \hat{P} = P. \tag{C15}$$

Equations (3) as well as the boundary condition $r_o/\rho_o = 1$ are satisfied by eqn (C15).

Finally, also note that the $\pm$ sign in eqn (C1) is included to handle possible changes in sign of the curvature at the equator of a highly inflated membrane. In particular, the sign is changed from positive to negative when $dr/d\rho = 0$, which occurs when $r\kappa_2$ becomes greater than unity for the first time.